MWMF-GLRW:Using Smart Model to Accurately Predict Non-coding RNA Interactions for Healthy Consumption

Tiyao Liu, Shudong Wang, Yawu Zhao, Xiaodong Tan, Shanchen Pang

***Abstract*—In the rapidly evolving field of consumer healthcare, the exploration of non-coding RNA interactions is crucial for drug development and personalized therapy. However, through traditional experimental validation methods, it is usually costly in terms of labor and money. In this article, we propose a efficient smart model utilizing multi-perspective weighted matrix factorization with global and local interactive-based random walk (MWMF-GLRW) to assist personalized treatment. First, only known interaction information was used to compute noncoding RNA similarities and perform fusions to ensure simplicity and generalizability of the model. Second, we innovatively develop a multi-perspective weighted matrix factorization technique. This method extracts key features while preserving the matrix structure, effectively enhancing the robustness and formative nature of miRNA-lncRNA edges between miRNA and lncRNA networks. Third, we introduce a new random walk method that considers both global information and local details of heterogeneous networks. This iterative interaction mechanism dynamically adjusts the model, enhancing its robustness and accuracy. Experiments show that MWMF-GLRW surpasses the state-of-the-art model on three datasets using only known interaction information. Notably, the simplicity of our methodology, combined with its high predictive efficiency, makes it well-suited for application in medical electronic devices aimed at promoting healthy patient consumption.**

***Index Terms*—non-coding RNA interactions, multi-perspective weighted matrix factorization, global and local interactive-based random walk, healthy Consumption.**

I. Introduction

Non-coding RNAs (ncRNAs) are a category of RNAs that do not encode proteins but engage in numerous cellular activities through interactions with other biomolecules [1, 2]. Among these, long non-coding RNAs (lncRNAs) and microRNAs (miRNAs) are particularly crucial regulators [3, 4]. Recent studies have highlighted the significant role of interactions between lncRNAs and miRNAs in cellular regulation [5]. LncRNAs can influence miRNA-mediated signaling pathways, thereby regulating the expression and function of related proteins [6]. For instance, the lncRNA HOTAIR interacts with miRNA-141 to regulate the expression and function of E-cadherin, a protein associated with breast cancer, thereby affecting cancer cell behavior [7].

In recent years, the application of artificial intelligence (AI) in smart consumer electronics and sustainable healthcare has achieved remarkable progress [8–11]. These technologies not only enhance user experience but also drive the development of personalized services. For instance, in smart consumer electronics, AI analyzes user habits and preferences to provide more accurate product recommendations and optimize smart home control [12, 13]. In the realm of sustainable healthcare, the integration of AI enables remote monitoring, disease prediction, and personalized treatment plans, significantly improving the efficiency and accessibility of healthcare services [14, 15]. In this article, we present an AI model designed to predict interactions between non-coding RNAs, which are crucial for elucidating disease mechanisms and have profound implications for health management and consumer electronics. Our intelligent models serve as a substitute for traditional bio-experimental validation methods, resulting in substantial savings in both labor and costs while informing the development of innovative health monitoring devices. These devices could utilize computational predictions to identify individuals at risk for certain diseases, thereby facilitating early intervention and more effective therapeutic strategies.

Molecular interactions can naturally form networks, with molecules and their interactions represented as nodes and edges, respectively. Molecular interaction networks are often combined with molecular similarity networks to create a heterogeneous network rich in information. In recent years, random walks on heterogeneous networks have proven effective in predicting molecular interactions [16–18]. Random walk is a probabilistic method that involves traversing from a specific node to neighboring nodes on a heterogeneous network to determine the potential association probability between the starting node and a target node [19]. However, the miRNA-lncRNA interaction network contains significant missing information, limiting the predictive power of current models. Matrix factorization is a useful technique to address this issue by complementing the miRNA-lncRNA interaction network [20]. Thus, matrix factorization can provide strong support for random walk. Despite this, existing matrix factorization methods struggle to adequately extract features of miRNAs and lncRNAs [20–22]. Additionally, current random walk models fail to account for both global information and local details within heterogeneous networks. Moreover, using multi-source data introduces challenges related to high noise levels

The research described in this work was supported by the National Key Research and Development Project of China (2021YF A1000102, 2021YF A1000103). (Corresponding author: Shudong Wang.)

Tiyao Liu, Shudong Wang, Yawu Zhao, Xiaodong Tan, and Shanchen Pang are with the College of Computer Science and Technology, Qingdao Institute of Software, China University of Petroleum (East China), Qingdao, Shandong 266580, China (e-mail: Z22070050@s.upc.edu.cn; shudongwang2013@sohu.com; zhaoyawu9608@163.com; pangsc@upc.edu.cn; reyes.tan@foxmail.com).

and increased model complexity in computational models.

To address the aforementioned limitations, we propose a prediction model for miRNA-lncRNA interactions using multi-perspective weighted matrix factorization with global and local interactive-based random walk (MWMF-GLRW). First, only using known interaction information, we compute the Gaussian and Laplace kernel similarity of miRNA/lncRNA and integrate these two similarities using similarity kernel fusion methods. This ensures both simplicity and generalization of the model. Second, we innovatively develop a multi-perspective weighted matrix factorization technique that incorporates miRNA and lncRNA multi-perspective similarities and their corresponding weighting matrices into the model. Third, we introduce a new random walk method that considers both global information and local details of heterogeneous networks. This iterative interaction mechanism dynamically adjusts the model, enhancing its robustness and accuracy.

The main contributions of this paper can be outlined as follows:

(1) Only using known interaction information, we compute the Gaussian kernel similarity and Laplace kernel similarity of miRNA/lncRNA and integrate these two similarities using similarity kernel fusion methods. This ensures both simplicity and generalization of the model. Notably, our newly introduced Laplace kernel similarity is more resistant to noise compared to Gaussian kernel similarity.

(2) We innovatively develop a multi-perspective weighted matrix factorization technique that incorporates miRNA and lncRNA multi-perspective similarities and their corresponding weighting matrices into the model. This method extracts key features while preserving the matrix structure, effectively enhancing the robustness and formative nature of miRNA-lncRNA edges between miRNA and lncRNA networks.

(3) We develop a global and local interactive-based random walk method. The global random walk captures key information on a broad scale, allowing for more accurate identification of important features. In contrast, the local random walk focuses on leveraging local networks to help the model understand complex molecular relationships and capture finer details. Additionally, the iterative interaction mechanism between the two facilitates dynamic adjustment of the model.

II. Related Work

A. Matrix factorization

Matrix factorization are often used to address interaction/association prediction challenges due to their simplicity and effectiveness in reconstructing missing entries in matrices.

Matrix factorization typically involves decomposing a large matrix into smaller, low-rank matrices. The product of these smaller matrices is then used to predict the missing entries in the original matrix. For example, HGIRCLMF [20] enhances the sparsity of biometric features by incorporating $L_{2,1}$-paradigm regularization into the objective function of matrix decomposition. DCMF [21] employs dual network co-matrix decomposition for predicting unknown small molecule (SM)-miRNA associations. PMFMDA [22] constructs a probabilistic matrix factorization algorithm using known association matrices and comprehensive similarity matrices to identify miRNAs potentially associated with diseases. However, existing matrix decomposition methods often overlook the geometric structure of the similarity data and cannot extract features adequately.

We develop a multi-perspective weighted matrix factorization technique that incorporates miRNA and lncRNA multi-perspective similarities and their corresponding weighting matrices into the model. This method extracts key features while preserving the matrix structure, effectively enhancing the robustness and formative nature of miRNA-lncRNA edges between miRNA and lncRNA networks.

B. Random Walk

Random walk is a probabilistic wandering from a specific node to neighboring nodes on a heterogeneous network to obtain the potential association probability between a specific node and a target node. Global random walk methods on heterogeneous networks are effective for interaction prediction. For example, IMSFHGI [23] initially employs a multi-similarity fusion approach to enhance the drug and target similarity. Subsequently, it utilizes heterogeneous graph inference to obtain the predicted scores. SLHGISMMA [24] first completes the missing values of the correlation network through sparse learning and then uses heterogeneous graph inference to obtain the predicted scores. On the other hand, local topology-based random walk methods focus on local network details. NTBiRW [16] constructs multiple microbial and disease similarity networks and integrates these through two-layer double random walks to obtain a final integrated network. Finally, weighted K-nearest neighbors were utilized for prediction. UBRW [25] uses a modified unbalanced double random walk technique to identify circRNA-disease associations. However, existing random walk models often fail to account for both global information and local details within heterogeneous networks.

We propose a global and local interactive-based random walk, which fully considers both the global information and local details of heterogeneous networks. Furthermore, the iterative interaction mechanism enables dynamic adjustment of the model.

III. METHODS

A. Gaussian kernel similarity

Due to its strong performance and broad applicability, the Gaussian kernel function is commonly used to calculate similarity between biological molecules [26–28]. In this study, we use the Gaussian kernel to compute the similarity between miRNAs and lncRNAs based on miRNA-lncRNA target pairs. Let $G(s_i)$ represents the vector containing the elements of row i in the miRNA-lncRNA interaction matrix $Y_{LM} \in R^{nl \times nm}$ (nl and nm denote the number of lncRNAs and miRNAs, respectively), and $G(m_j)$ indicates the vector containing the elements of column j in Y_{LM}. The calculation equations are presented below:

$$Y_{MM}^{1}(m_i, m_j) = exp\left(-q_m \left\|G(m_i) - G(m_j)\right\|^2\right) \quad (1)$$

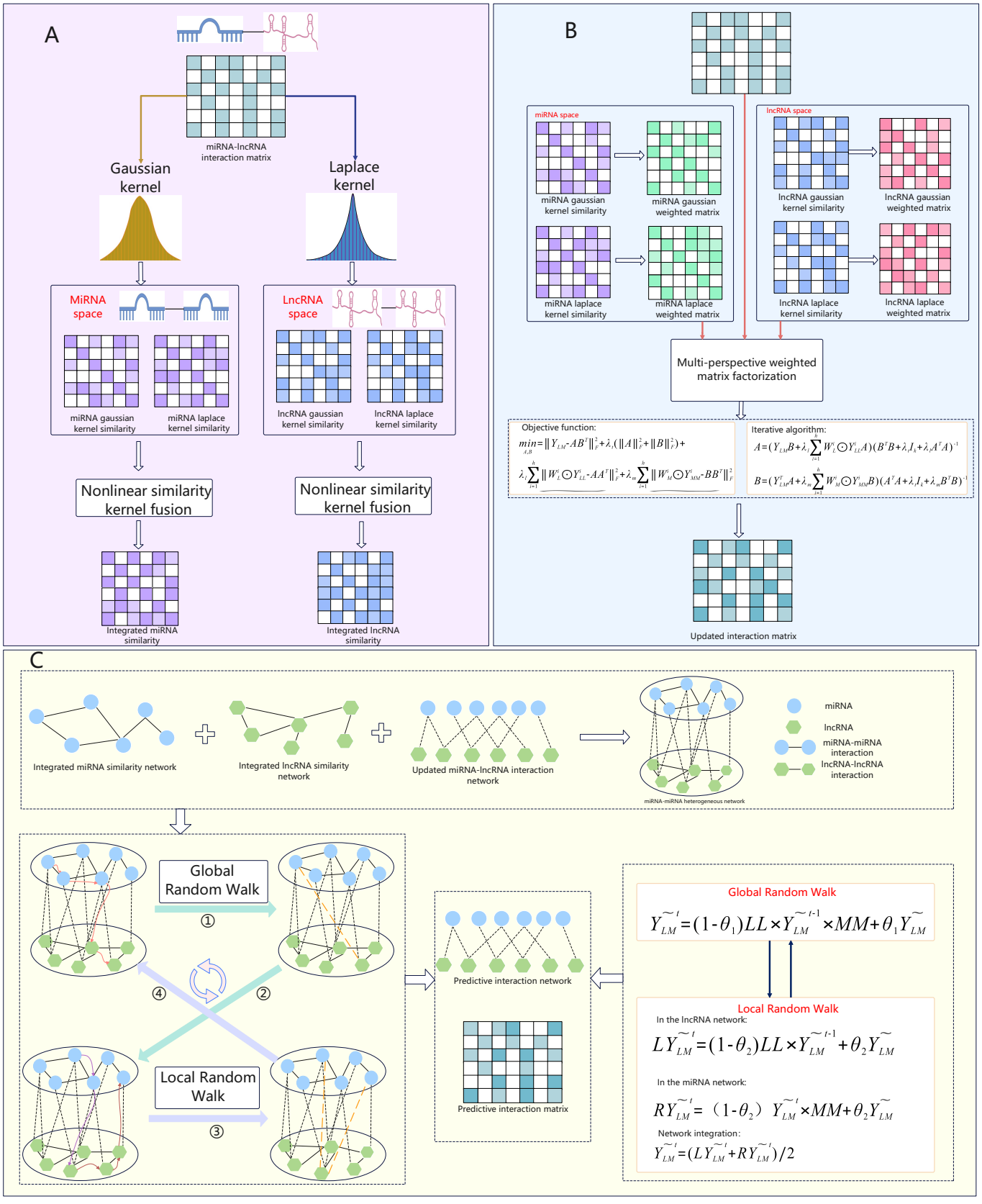

(a)

Fig. 1. Framework of MWMF-GLRW. (A) The Gaussian and Laplace kernel similarities of miRNAs/lncRNAs were calculated, and different types of similarities were integrated using nonlinear fusion methods. (B) The multi-view similarity of miRNAs and lncRNAs and their corresponding weighted matrices were incorporated into the model to fill in the missing information of the interaction matrix. (C) Using a global and local interactive random walk algorithm to obtain predictions.

$$Y_{LL}^{1}(l_i, l_j) = exp\left(-q_l \left\|G(l_i) - G(l_j)\right\|^2\right) \quad (2)$$

where Y_{MM}^{1} denotes the Gaussian kernel similarity between miRNAs, and Y_{LL}^{1} indicates the Gaussian kernel similarity between lncRNAs. The adjustable parameters q_m and q_l are defined by the following equations:

$$q_m = 1/\frac{1}{nm}\sum_{i=1}^{nm} \left\|G(m_i)\right\|^2 \quad (3)$$

$$q_l = 1/\frac{1}{nl}\sum_{i=1}^{nl} \left\|G(l_i)\right\|^2 \quad (4)$$

B. Laplace kernel similarity

While the Gaussian kernel function performs well in many scenarios, the Laplace kernel function is particularly advantageous for handling noisy and high-dimensional data [29]. Therefore, we innovatively introduce the Laplace kernel function to compute the Laplace similarity between miRNAs and between lncRNAs. Let $L(m_i)$ indicates the vector containing the elements of row i in Y_{LM} and $L(l_j)$ signifies the vector containing the elements of column j in Y_{LM}. The calculation equations are presented below:

$$Y_{MM}^{2}(m_i, m_j) = exp(\frac{\left\|L(m_i) - L(m_j)\right\|}{-\sigma}) \quad (5)$$

$$Y_{LL}^{2}(l_i, l_j) = exp(\frac{\left\|L(l_i) - L(l_j)\right\|}{-\sigma}) \quad (6)$$

where Y_{MM}^{2} denotes the Laplace kernel similarity between miRNAs, and Y_{LL}^{2} represents the Laplace kernel similarity between lncRNAs. The parameter σ is employed to regulate the function bandwidth. In this research, we consistently set the parameter σ to a value of 2.

C. Similarity kernel fusion

We now have two types of similarity kernels for miRNAs (miRNA Gaussian kernel similarity and miRNA Laplace kernel similarity) and two types for lncRNAs (lncRNA Gaussian kernel similarity and lncRNA Laplace kernel similarity).

Here, the similarity kernel fusion method was used to integrate two miRNA similarity kernels (Y_{MM}^{1} and Y_{MM}^{2}). In the first step, we standardize each miRNA similarity kernels as detailed below:

$$P_h(i, j) = \frac{Y_{MM}^{h}(i, j)}{\sum_{k=1}^{nm} Y_{MM}^{h}(k, j)} \quad (7)$$

In the second step, we construct a neighborhood constraint kernel for Y_{MM}^{1} and Y_{MM}^{2} to efficiently capture the local similarity of miRNAs.

$$S_h(i, j) = \begin{cases} \frac{Y_{MM}^{h}(i,j)}{\sum_{k\in N_i} Y_{MM}^{h}(i,k)} & j \in N_i \\ 0 & otherwise \end{cases} \quad (8)$$

where S_h denotes a neighbor-constraint kernel. Here, the neighbor set N_i of miRNA m_i is characterized as the k most similar miRNAs to m_i.

In the third step, we combine the normalized similarity kernel P_h and the neighbor-constraint kernel S_h literally, as detailed below:

$$P_h^{t+1} = \alpha(S_h \times \frac{\sum_{r\neq h} P_r^t}{2} \times S_h^T) + (1-\alpha)\frac{\sum_{r\neq h} P_r^0}{2} \quad (9)$$

where P_h^{t+1} indicates the h-th kernel acquired after t-th iterations, P_r^0 denotes the initial value of P_r^t, and $\alpha \in (0, 1)$ indicates the equilibrium coefficient. After t-th iterations, the final kernel is derived the following:

$$SM = \frac{1}{2}\sum_{h=1}^{2} P_h^{t+1} \quad (10)$$

In the fourth step, a weighted matrix is added on top of embedding more neighbor information. The formula is detailed below.

$$w(i, j) = \begin{cases} 1 & if\ i \in N_j \cap j \in N_i \\ 0 & if\ i \notin N_j \cap j \notin N_i \\ 0.5 & otherwise \end{cases} \quad (11)$$

Finally, we obtain the integrated miRNA similarity kernel matrix $MM \in R^{nm*nm}$ as follows:

$$MM = w(i, j) * SM \quad (12)$$

Similarly, we obtain the integrated lncRNA similarity kernel matrix $LL \in R^{nl*nl}$.

D. Multi-perspective weighted matrix factorization

In this work, we present a novel multi-perspective weighted matrix factorization technique to populate the miRNA-lncRNA interaction network. To fully explore miRNA/lncRNA features from different similarity perspectives while preserving the self-similarity structure, we introduce multi-perspective similarity in the matrix factorization process and compute their nearest-neighbor graphs as weight matrices. This multi-perspective weighted matrix factorization is primarily applied to different similarity matrices in both the miRNA and lncRNA spaces. For miRNAs: $Y_{MM} = \left\{Y_{MM}^{1}, Y_{MM}^{2}, \ldots, Y_{MM}^{h}\right\}$ and for lncRNAs: $Y_{LL} = \left\{Y_{LL}^{1}, Y_{LL}^{2}, \ldots, Y_{LL}^{h}\right\}$, where h indicates the number of similarity perspectives. First, we utilize the similarity matrix neighbor information of the two perspectives (Gaussian-based and Laplace-based) in miRNA space and lncRNA space to compute the corresponding weight matrices of each similarity matrix, respectively. Then, we multiply the different perspective similarities in the miRNA space with their corresponding weight matrices and compare them with the product of the miRNA potential feature vectors. Similar operations are performed in the lncRNA space. Finally, these components are incorporated into the objective function of the standard matrix factorization to construct a multi-perspective weighted matrix factorization model.

Step 1 (Compute the weight matrix):

First, we find the corresponding weight matrix for each similarity using the neighbor information of similarity matrices W_M^1 and W_M^2 under miRNA space, respectively.

$$W_M^h(i,j) = \begin{cases} 1 & if\ i \in N_j^{'} \cap j \in N_i^{'} \\ 0 & if\ i \notin N_j^{'} \cap j \notin N_i^{'} \\ 0.5 & otherwise \end{cases} \tag{13}$$

Here, $N_i^{'}$ denotes the set of neighbors of miRNA m_i. W_M^h denotes the similarity weight matrix under miRNA space. The same process is applied to the lncRNA space, yielding the lncRNA similarity weight matrix W_L^h.

Step 2 (Implement multi-perspective weighted matrix factorization): The primary purpose of matrix factorization is to decompose a large matrix into two smaller matrices A and B, where $Y_{LM} \approx AB^T$. Subsequently, we formulate the objective function for multi-perspective weighted matrix factorization utilizing the matrices A and B as follows:

$$\min_{\mathrm{A,B}} = \left\| Y_{LM} - AB^T \right\|_F^2 + \lambda_t \left(\|A\|_F^2 + \|B\|_F^2 \right) + \lambda_l \sum_{i=1}^{h} \left\| W_L^i \odot Y_{LL}^i - AA^T \right\|_F^2 + \lambda_m \sum_{i=1}^{h} \left\| W_M^i \odot Y_{MM}^i - BB^T \right\|_F^2 \tag{14}$$

where $\|\cdot\|_F$ indicates Frobenius norm and λ_t, λ_l, λ_m are non-negative parameters. The first entry represents an approximate model of the matrix Y_{LM}, aiming to identify the latent feature matrices A and B. The second entry serves as Tikhonov regularization, minimizing the norm of A and B to prevent overfitting. The third and fourth terms impose regularization constraints and weighting constraints to ensure that the miRNA/lncRNA similarity is more similar to their underlying feature vectors while the underlying structure of the similarity matrix remains unchanged.

Furthermore, to acquire the initial value of A and B, we utilize the singular value decomposition method on the matrix Y_{LM} as follows:

$$[U,S,V] = SVD(Y_{LM},k), A = US_k^{1/2}, B = VS_k^{1/2} \quad where\ Y_{LM} = U * S_k * V \tag{15}$$

where S_k contains the k largest singular values of Y_{LM} and $U \in R^{ns*k}$/$V \in R^{k*nm}$ contains the associated singular vectors.

We use the alternating least squares approach to solve the optimization problem in equation (20). First, we denote equation (20) as L. Then, by setting $\partial L/\partial A = 0$ and $\partial L/\partial B = 0$, we iteratively update A and B until convergence. The iterative formulas for updating A and B are given as follows:

$$A = (Y_{LM}B + \lambda_l \sum_{i=1}^{h} W_L^i \odot Y_{LL}^i A)(B^T B + \lambda_t I_k + \lambda_l A^T A)^{-1} \tag{16}$$

$$B = (Y_{LM}^T A + \lambda_m \sum_{i=1}^{h} W_M^i \odot Y_{MM}^i B)(A^T A + \lambda_t I_k + \lambda_m B^T B)^{-1} \tag{17}$$

where I_k represents a diagonal matrix of dimension k with all diagonal elements set to 1. Finally, the populated miRNA-lncRNA interaction matrix $\tilde{Y_{LM}} = AB^T$ can be acquired. The specific algorithm for the multi-perspective weighted matrix factorization is detailed in Algorithm 1.

Algorithm 1 Multi-perspective Weighted Matrix Factorization

Require: Y_{LM}, Y_{MM}^1, Y_{MM}^2,Y_{LL}^1,Y_{LL}^2, λ_t, λ_l, λ_m
Ensure: $\tilde{Y_{LM}}$
1: $[U,S,V] = SVD(Y_{LM},k), A = US_k^{1/2}, B = VS_k^{1/2}$
2: **Repeat**
3: Update A: $A = (Y_{LM}B + \lambda_l \sum_{i=1}^{h} W_L^i \odot Y_{LL}^i A)(B^T B + \lambda_t I_k + \lambda_l A^T A)^{-1}$
4: Update B: $B = (Y_{LM}^T A + \lambda_m \sum_{i=1}^{h} W_M^i \odot Y_{MM}^i B)(A^T A + \lambda_t I_k + \lambda_m B^T B)^{-1}$
5: **Until convergence**
6: **return** $\tilde{Y_{LM}} = AB^T$

E. Global and local interactive-based random walk

Previous random walk algorithms on heterogeneous networks have not fully considered both the global information and local details of such networks [16, 23–25]. Here, we develop a global and local interactive-based random walk algorithm to predict unknown miRNA-lncRNA interactions. The global random walk focuses on the entire miRNA-lncRNA heterogeneous network, allowing the capture of key information on a global scale and the accurate identification of crucial features. In contrast, the local random walk leverages the miRNA and lncRNA networks to help the model understand the complex relationships between molecules and capture local details more effectively. This combination harnesses the strengths of both approaches, enhancing the model's performance and accuracy. Additionally, the iterative interaction mechanism between the two enables dynamic adjustment of the model.

We can utilize the well-established miRNA-lncRNA interaction network, the integrated miRNA similarity network, and the integrated lncRNA similarity network to construct an enriched miRNA-lncRNA heterogeneous network. Let L = $\{L_1, L_2, \ldots, L_{nl}\}$ represent nl lncRNA nodes and M = $\{M_1, M_2, \ldots, M_{nm}\}$ represent nm miRNA nodes. We let E_{ll}, E_{mm}, E_{lm} represent lncRNA-lncRNA, miRNA-miRNA and lncRNA-miRNA edges, respectively, and W_{ll}, W_{mm}, W_{lm} indicate the weights on these three edges. Then the miRNA-lncRNA heterogeneity graph was represented as $G_{LM} = \{\{L, M\}, \{E_{ll}, E_{mm}, E_{lm}\}, \{W_{ll}, W_{mm}, W_{lm}\}\}$.

MWMF-GLRW first performs global random walk over the entire heterogeneous network, and then performs simultaneous local random walk from the miRNA network and the lncRNA network. Finally, the global and local random walks are performed interactively, feeding into each other to achieve a comprehensive prediction score.

Step 1 (Compute the initial transition probability): Begin by normalizing the similarity network using the following formula:

$$LL(i,j) = \frac{LL(i,j)}{\sqrt{\sum_{q=1}^{nl} LL(i,q) \sum_{q=1}^{nl} LL(q,j)}} \tag{18}$$

$$MM(i,j) = \frac{MM(i,j)}{\sqrt{\sum_{q=1}^{nl} MM(i,q) \sum_{q=1}^{nl} MM(q,j)}} \tag{19}$$

TABLE I
THE DETAILS OF SELECTED DATASETS ARE IN THIS PAPER.

Dadasets	Data Source	RNAs/SMs	RNAs/Diseases	Associations	Sparsity
Benchmark dataset	lncRNASNP	780	275	5118	0.0239
SM-miRNA dataset	SM2miR v1.0	39	286	664	0.0595
MiRNA-disease dataset	HMDD v2.0	495	383	5430	0.0286

Step 2 (Perform global random walk): MWMF-GLRW performs global random walk over the entire miRNA-lncRNA heterogeneous network with the following formula:

$$\tilde{Y_{LM}}^{t} = (1-\theta_1)LL \times \tilde{Y_{LM}}^{t-1} \times MM + \theta_1 \tilde{Y_{LM}} \quad (20)$$

Here, $\tilde{Y_{LM}}$ represents the predicted results via global random walk over the entire heterogeneous network. θ_1 denotes the restart probability of global random walk.

Step 3 (Perform local random walk): Incorporate the output of the global random walk into the local random walk module. Subsequently, MWMF-GLRW performs local random walks on miRNA and lncRNA network, respectively. The equation is shown below.

In the lncRNA network:

$$\tilde{LY_{LM}}^{t} = (1-\theta_2)LL \times \tilde{Y_{LM}}^{t-1} + \theta_2 \tilde{Y_{LM}} \quad (21)$$

In the miRNA network:

$$\tilde{RY_{LM}}^{t} = (1-\theta_2)\tilde{Y_{LM}}^{t-1} \times MM + \theta_2 \tilde{Y_{LM}} \quad (22)$$

where $\tilde{LY_{LM}}$ and $\tilde{RY_{LM}}$ represent the predicted results via local random walks over the lncRNA network and the miRNA network, respectively. θ_2 is the restart probability of local random walk. Considering the different topological and structural characteristics of lncRNA network and miRNA network, we set l and m as the maximum number of iterations for lncRNA network and miRNA network, respectively. The average output $\tilde{Y_{LM}}^{t}$ of the lncRNA network and miRNA network at each step during the iteration process is used as the local random walk result. The formula is detailed below.

$$\tilde{Y_{LM}}^{t} = (\tilde{LY_{LM}}^{t} + \tilde{RY_{LM}}^{t})/2 \quad (23)$$

Then, the local random walk results from each iteration are fed back into the global random walk module to form an interactive model, enhancing the overall prediction performance.

F. MWMF-GLRW

The complete flowchart of MWMF-GLRW is illustrated in Fig.1. Our models framework can be outlined in three steps. First, only using known interaction information, we compute the Gaussian and Laplace kernel similarity of miRNA/lncRNA and integrate these two similarities using similarity kernel fusion method. Second, we innovatively develop a multi-perspective weighted matrix factorization technique that incorporates miRNA and lncRNA multi-perspective similarities and their corresponding weighting matrices into the model. Third, we introduce a new random walk method that considers both the global information and local details of heterogeneous networks. The iterative interaction mechanism realizes the dynamic adjustment of the model. Algorithm 2 describes the workflow of the MWMF-GLRW method.

Algorithm 2 MWMF-GLRW

Require: $\tilde{Y_{LM}}$, LL, MM, θ
Ensure: F

```
Calculate miRNA/lncRNA Gaussian kernel similarity using only known interaction information;
Calculate miRNA/lncRNA Laplace kernel similarity using only known interaction information;
Integrate miRNA and lncRNA for Gaussian and Laplacean kernel similarity using similarity kernel fusion method;
Complete the miRNA-lncRNA association network using multi-perspective weighted matrix factorization method;
//Iteration process;
max_iter = max([l, m]);
for t = 1 : max_iter;
    Lflag = 0;
    Mflag = 0;
    //Global random walk in lncRNA network;
    Y~_LM^t = (1-θ1)LL × Y~_LM^(t-1) × MM + θ1 Y~_LM;
    //Local random walk in lncRNA network;
    if(t ≤ l);
        Lflag = 1;
        LY~_LM^t = (1-θ2)LL × Y~_LM^(t-1) + θ2 Y~_LM;
    endif;
    //Local random walk in miRNA network;
    if(t ≤ m);
        Mflag = 1;
        RY~_LM^t = (1-θ2) Y~_LM^(t-1) × MM + θ2 Y~_LM ;
    endif;
    Y~_LM^t = (LY~_LM^t + RY~_LM^t)/2;
end
F=Y~_LM^t;
return F
```

IV. RESULTS AND DISCUSSION

In this section, we first describe the experimental setup and then compare our model, MWMF-GLRW, with the baseline for miRNA-lncRNA interaction prediction. Additionally, we investigate the model's generalization ability to predict molecular interactions. Subsequently, we conduct a parametric analysis to determine the optimal parameters and perform ablation experiments to validate the effectiveness of the modules. Finally, we further validate the practical applicability of the model's predictions through two case studies.

A. Experimental Settings

Datasets. Since MWMF-GLRW only requires known associations as input, it can efficiently handle various types of datasets. We conducted experiments on three distinct datasets:

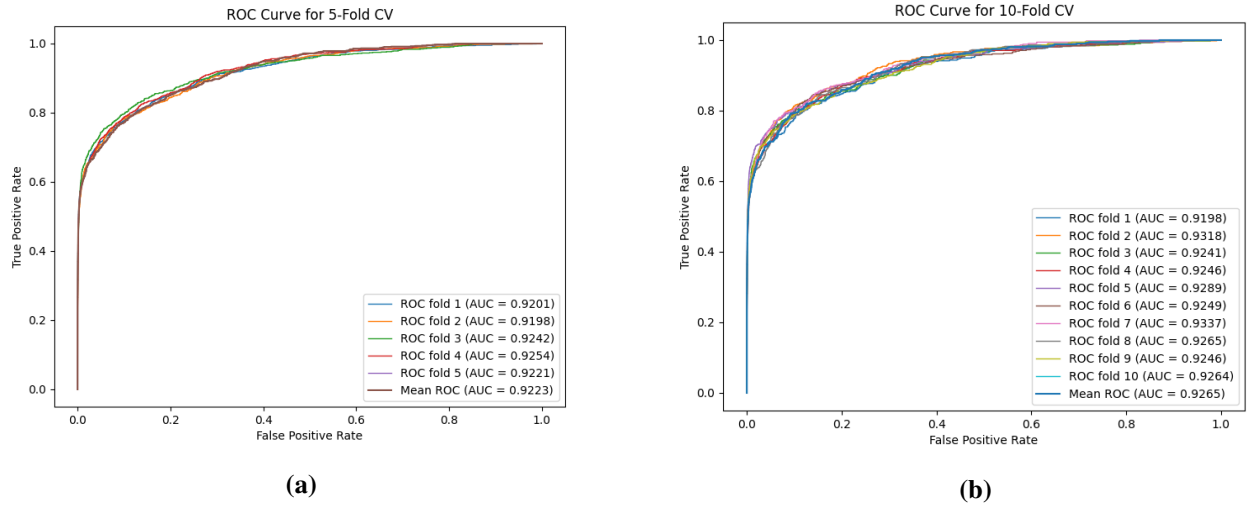

(a) **(b)**

Fig. 2. (a) MWMF-GLRW executes 5-fold CV on the benchmark dataset; (b) MWMF-GLRW executes 10-fold CV on the benchmark dataset.

TABLE II
MULTIPLE METRICS RESULTS OBTAINED BY MVPFDPC ON THE BASELINE DATASET USING 5-FOLD CV

Fold	Accuracy	Precision	Recall	F1-score	MCC
1	0.9113	0.7578	0.6875	0.7209	0.6695
2	0.9197	0.7840	0.7158	0.7483	0.7017
3	0.9122	0.7610	0.6904	0.7240	0.6731
4	0.9134	0.7689	0.6862	0.7252	0.6755
5	0.9129	0.7635	0.6911	0.7255	0.6751
Average	0.9139	0.7670	0.6942	0.7288	0.6790

TABLE III
PERFORMANCE COMPARISON OF MWMF-GLRW WITH SEVERAL METHODS IN BENCHMARK DATASET.

Method	EPLMI	INLMI	LMNLMI	LNRLMI	LCBNI	GKLOMLI	MWMF-GLRW
AUC	0.8447	0.8517	0.8926	0.8960	0.8982	0.9053	0.9223

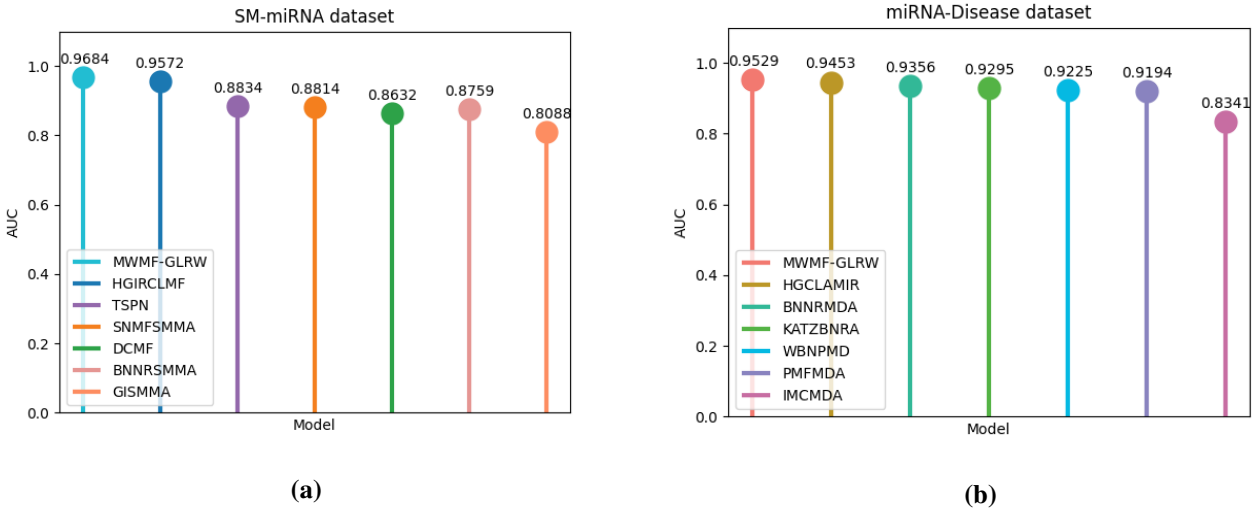

(a) **(b)**

Fig. 3. Performance comparison of MWMF-GLRW with several methods in SM-miRNA dataset and miRNA-Disease dataset.

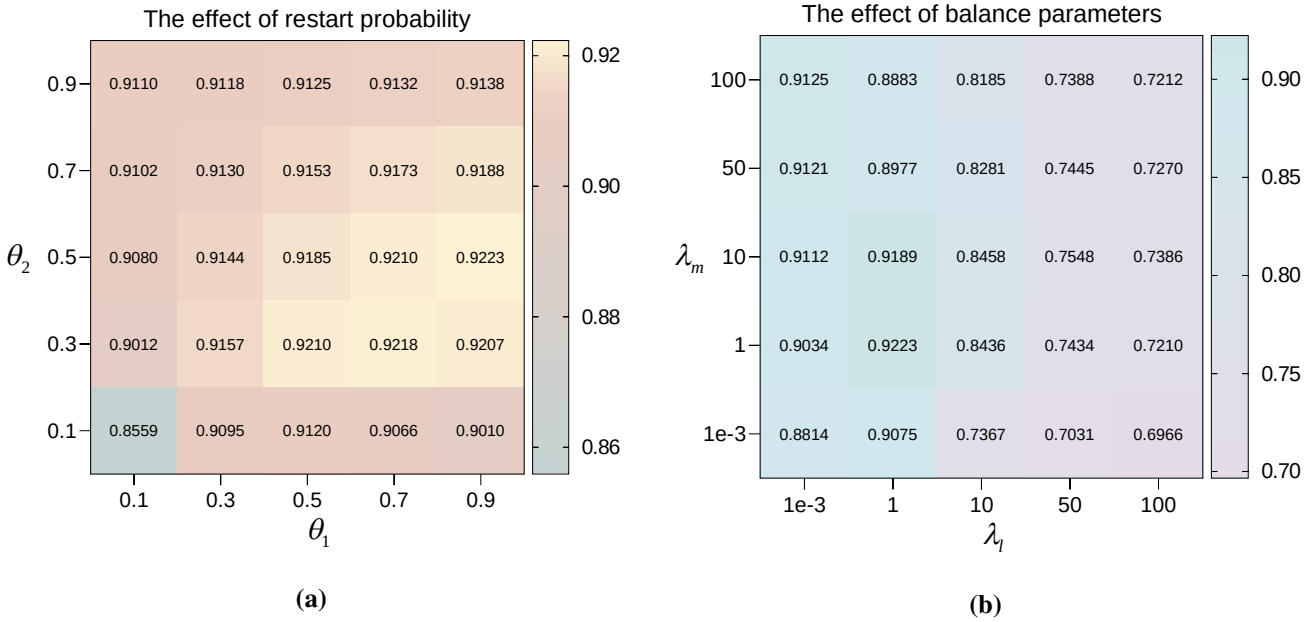

Fig. 4. The parameter sensitivity analysis.

miRNA-lncRNA, SM-miRNA, and miRNA-disease. For the miRNA-lncRNA dataset, we obtained 5,118 interactions involving 275 miRNAs and 780 lncRNAs from the lncRNASNP database [30], which serves as our benchmark dataset. Additionally, we collected 664 SM-miRNA associations involving 39 SMs and 286 miRNAs from SM2miR v1.0 [31]. For the miRNA-disease dataset, we gathered 5,430 associations involving 495 miRNAs and 383 diseases from HMDD v2.0 [32]. Detailed information on all datasets used in our study is provided in Table I. Notably, all these datasets exhibit high sparsity, with many unknown associations, highlighting the need for effective methods to populate the molecular interaction/association networks.

Baselines. We compare our proposed MWMF-GLRW with several baseline methods using the benchmark dataset, which are categorized as follows:

• GKLOMLI [33] outputs miRNA and lncRNA similarity matrices using a Gaussian kernel-based approach. It then infers miRNA-lncRNA interactions by applying a linearly optimized link prediction model to these similarity matrices and known interaction networks.

• LCBNI [34] introduces a link-complementary bipartite network inference approach to predict potential miRNA-lncRNA interactions.

• LNRLMI [35] integrates known interaction networks to construct a two-part network based on the similarity of lncRNA and miRNA expression profiles. It then employs a linear neighbor representation within this network to develop a prediction model.

• LMNLMI [36] employs network fusion techniques to merge multiple similarity networks and applies matrix completion methods to predict interactions.

• INLML [37] integrates expression and sequence similarity networks and predicts interaction scores using matrix decomposition techniques.

• EPLMI [38] constructs a bipartite graph that incorporates miRNA similarity, lncRNA similarity, and miRNA-lncRNA interactions. The predicted scores are then derived using graphical inference techniques.

Implementation details and evaluation metrics. To validate MWMF-GLRW's predictive performance, we implemented 5-fold and 10-fold crossvalidation (CV) experiments on two datasets. The datasets are randomly divided into 5 parts and 10 parts, leaving one part as the test set and the rest as the training set for each experiment. This approach helps mitigate the impact of dataset division randomness on the experimental results.

Additionally, we employed seven commonly used evaluation metrics in our study: area under the receiver operating characteristic (ROC) curve (AUC), accuracy, precision, recall, F1-score, and Matthews correlation coefficient (MCC).

B. Performance Evaluation

In this work, we assessed the predictive capability of MWMF-GLRW using both 5-fold and 10-fold CV on the benchmark dataset. As shown in Fig. 2, MWMF-GLRW achieved impressive AUC values of 0.9223 and 0.9265 for 5-fold and 10-fold CV, respectively. To provide a comprehensive evaluation of MWMF-GLRWs performance, we employed multiple metrics. To ensure a balanced assessment of positive and negative samples, we maintained a 1:1 ratio of positive to negative samples. As detailed in Table II, MWMF-GLRW achieved mean values of 0.9139 for accuracy, 0.7670 for precision, 0.6942 for recall, 0.7288 for F1-score, and 0.6790 for MCC. Based on these results, it is evident that MWMF-GLRW demonstrates outstanding predictive capabilities.

To further assess the effectiveness of MWMF-GLRW, we compare it with six recent models: GKLOMLI, LCBNI, LNRLMI, LMNLMI, INLMI, and EPLMI. For a fair comparison, we use the commonly employed AUC metric to assess

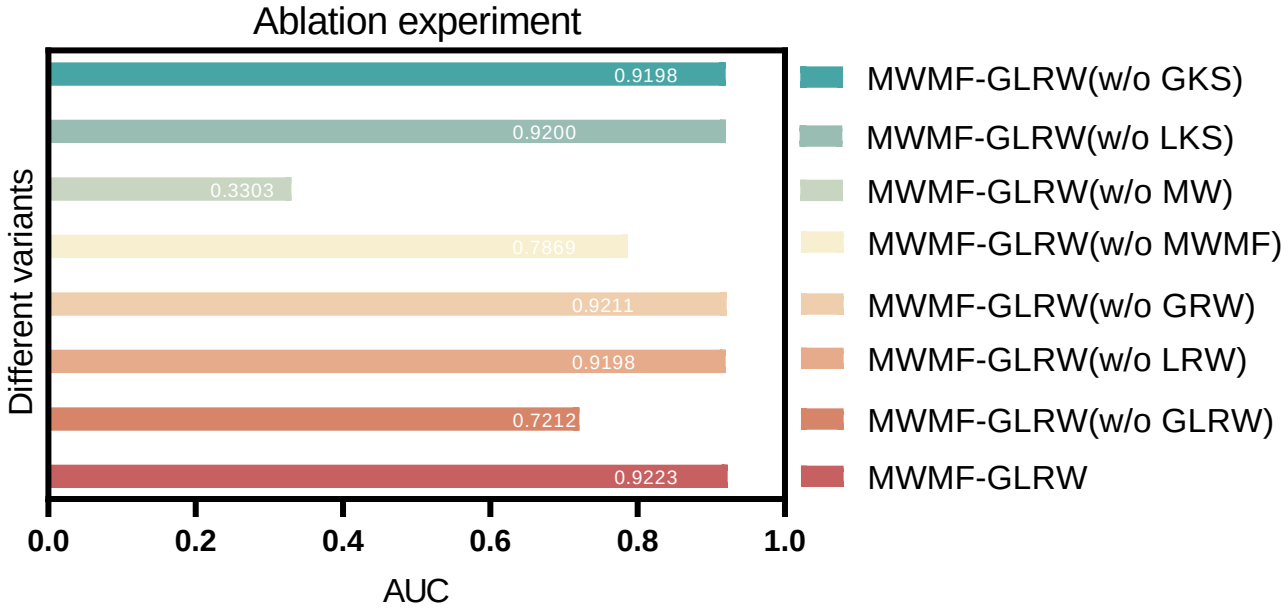

(a)

Fig. 5. Results of ablation experiments.

the average performance of each model from 5-fold cross-validation on benchmark dataset. The results are summarized in Table III. MWMF-GLRW consistently outperforms the other models, achieving an AUC that is 0.0776, 0.0706, 0.0297, 0.0263, 0.0241, and 0.017 higher than EPLMI, INLMI, LMNLMI, LNRLMI, LCBNI, and GKLOMLI, respectively.

C. Generalized Molecular Interaction/Association Prediction Study

MWMF-GLRW requires less data while effectively integrating matrix factorization and random walk techniques to achieve accurate molecular interaction predictions. We applied MWMF-GLRW to both the SM-miRNA and miRNA-disease datasets and compared its performance with several state-of-the-art models to assess its generalizability. For the SM-miRNA dataset, we compared MWMF-GLRW with models such as HGIRCLMF [20], TSPN [39], SNMFSMMA [40], DCMF [41], BNNRSMMA [42], and GISMMA [43]. Similarly, for the miRNA-disease dataset, we compared it with HGCLAMIR [44], BNNRMDA [45], KATZBNRA [46], WBNPMD [47], PMFMDA [48], and IMCMDA [49]. As shown in Figure 3, MWMF-GLRW achieved AUC values of 0.9684 for the SM-miRNA dataset and 0.9529 for the miRNA-disease dataset, surpassing the AUCs of the other models in their respective domains. These results indicate that MWMF-GLRW demonstrates strong generalizability in the field of molecular interaction prediction.

D. Parameter sensitivity analysis

In this section, we conduct a parameter sensitivity analysis to examine how several key parameters impact the performance of MWMF-GLRW. Specifically, we analyze the effects of the restart probabilities θ_1 and θ_2, as well as the coefficients λ_l and λ_m in Eq. (14).

The effect of restart probability θ_1 and θ_2. We vary the restart probabilities θ_1 and θ_2 for different random walks, testing values in the range $0.1, 0.3, 0.5, 0.7, 0.9$. Results shown in Figure 4(a) indicate that MWMF-GLRW performs best with $\theta_1 = 0.9$ and $\theta_2 = 0.5$. Consequently, we set 0.9 and 0.5 as the restart probabilities for the global and local random walks, respectively.

The effect of balance parameters λ_l and λ_m. We vary the coefficients λ_l and λ_m in Eq. (14) to investigate their impact on the contribution of different biological features. Specifically, λ_l and λ_m are tested within the range $1e-3, 1, 10, 50, 100$. The results show that MWMF-GLRW achieves the best performance with $\lambda_l = 1$ and $\lambda_m = 1$. Analyzing the results presented in Figure 4(b), we observe the following: (1) Larger values of λ_l and λ_m tend to reduce model performance. This is because excessively high weights on biosimilarity features cause the model to overly rely on similarity accuracy during training, leading to underutilization of the known interaction information. (2) Optimal performance is achieved when λ_l equals λ_m, indicating that the contributions of miRNA similarity features and lncRNA similarity features to the model's performance are approximately equal.

E. Ablation Study

To evaluate the importance of various components in our model, we examine the following variants of MWMF-GLRW:

- MWMF-GLRW without Gaussian kernel similarity (w/o GKS) removes Gaussian kernel similarity from MWMF-GLRW.
- MWMF-GLRW without Laplace kernel similarity (w/o LKS) removes Laplace kernel similarity from MWMF-GLRW.

• MWMF-GLRW without the multi-view weighting property (w/o MW) removes the multi-view weighting property from the matrix factorization and directly uses the normal matrix factorization.

• MWMF-GLRW without multiview weighting matrix decomposition (w/o MWMF) removes the multiview weighting matrix decomposition from MWMF-GLRW.

• MWMF-GLRW without global random walk (w/o GRW) removes the global random walk and uses local random walk directly for prediction.

• MWMF-GLRW without local random walk (w/o LRW) removes the global random walk and uses global random walk directly for prediction.

• MWMF-GLRW without global and local interactive-based random walk (w/o GLRW) removes the global and local interactive-based random walk.

As illustrated in Figure 5 (with AUCs macro-averaged), all variants of MWMF-GLRW show a decrease in performance, confirming that each component contributes to the prediction of miRNA-lncRNA interactions. The observations are as follows: (1) MWMF-GLRW (w/o GKS) and MWMF-GLRW (w/o LKS) exhibit reduced prediction performance, indicating that the integration of Gaussian kernel similarity and Laplace kernel similarity enhances predictive ability. The fact that MWMF-GLRW (w/o GKS) outperforms MWMF-GLRW (w/o LKS) suggests that the newly proposed Laplace kernel similarity has greater importance than Gaussian kernel similarity. (2) MWMF-GLRW outperforms both MWMF-GLRW (w/o MW) and MWMF-GLRW (w/o MWMF), indicating that the multi-view weighted matrix decomposition is valuable for predicting miRNA-lncRNA interactions. (3) MWMF-GLRW surpasses MWMF-GLRW (w/o GRW) and MWMF-GLRW (w/o LRW), suggesting that the interactive global and local random walks provide superior results compared to using global or local random walks alone. Additionally, this highlights that local details are more critical than the global structure. (4) MWMF-GLRW performs better than both MWMF-GLRW (w/o MWMF) and MWMF-GLRW (w/o GLRW), demonstrating that the integration of multi-view weighting matrix decomposition and interactive random walks significantly enhances miRNA-lncRNA interaction prediction.

F. Case studies

To further assess the practical inferential capability of MWMF-GLRW, we selected two lncRNAs (lnc-WWP2-2:1 and lnc-DPM1-1:1) from the benchmark dataset as case studies. We removed the known interactions involving these lncRNAs, prioritized all relevant miRNAs based on MWMF-GLRW predictions, and validated them by comparing with the top 10 most relevant miRNAs in a well-established MLI database [30]. In Table IV, 9 out of the top 10 miRNAs associated with lnc-WWP2-2:1 are confirmed by the database. Table V lists the miRNAs related to lnc-DPM1-1:1 inferred by MWMF-GLRW. Thus, we accurately predicted 9 out of the top 10 miRNAs for both lncRNAs, demonstrating the practical effectiveness of our model.

TABLE IV
TOP 10 MIRNAS PREDICTED BY MWMF-GLRW TO BE CONNECTED TO LNC-WWP2-2:1

Rank	miRNA	Evidence
1	hsa-miR-29b-3p	lncRNASNP
2	hsa-miR-29c-3p	lncRNASNP
3	hsa-miR-29a-3p	lncRNASNP
4	hsa-miR-181c-5p	lncRNASNP
5	hsa-miR-181a-5p	lncRNASNP
6	hsa-miR-181b-5p	lncRNASNP
7	hsa-miR-181d-5p	lncRNASNP
8	hsa-miR-4262	unknown
9	hsa-miR-1	lncRNASNP
10	hsa-miR-203a	lncRNASNP

TABLE V
TOP 10 MIRNAS PREDICTED BY MWMF-GLRW TO BE CONNECTED TO LNC-DPM1-1:1

Rank	miRNA	Evidence
1	hsa-miR-424-5p	lncRNASNP
2	hsa-miR-15b-5p	lncRNASNP
3	hsa-miR-195-5p	lncRNASNP
4	hsa-miR-15a-5p	lncRNASNP
5	hsa-miR-497-5p	lncRNASNP
6	hsa-miR-16-5p	lncRNASNP
7	hsa-miR-214-3p	lncRNASNP
8	hsa-miR-761	lncRNASNP
9	hsa-miR-3619-5p	lncRNASNP
10	hsa-miR-503-5p	unknown

V. CONCLUSION

By utilizing intelligent models to accurately predict non-coding RNA interactions, we can inform the design of health-monitoring devices and leverage this information to offer personalized health advice, ultimately promoting healthy patient consumption. Our approach leverages only known relevant information to compute kernel similarities, ensuring both model simplicity and generalizability. Notably, our newly introduced Laplace kernel similarity proves to be more resilient to noise compared to Gaussian kernel similarity. MWMF-GLRW extracts key features while maintaining the matrix structure, effectively enhancing the robustness and formation of miRNA-lncRNA edges within both miRNA and lncRNA networks. Furthermore, the framework comprehensively considers both global information and local details of heterogeneous networks, with an iterative interaction mechanism that allows dynamic model adjustments. Extensive experiments on three datasets show that MWMF-GLRW consistently surpasses current state-of-the-art models. Additionally, two case studies further validate the efficacy of our approach.

In future work, we plan to address several areas for improvement. First, the limited number of known interactions constrains the model's predictive power; thus, we aim to enhance the interaction matrix using deep learning techniques. Second, there is a need for a more in-depth exploration of miRNA-lncRNA interaction mechanisms, and we intend to integrate these mechanisms into our model to advance its predictive accuracy.

REFERENCES

[1] A. Caporali, M. Anwar, Y. Devaux, R. Katare, F. Martelli, P. K. Srivastava, T. Pedrazzini, and C. Emanueli, "Non-

coding rnas as therapeutic targets and biomarkers in ischaemic heart disease," Nature Reviews Cardiology, pp. 1–18, 2024.
[2] A. Fatica and I. Bozzoni, "Long non-coding rnas: new players in cell differentiation and development," Nature Reviews Genetics, vol. 15, no. 1, pp. 7–21, 2014.
[3] D. P. Bartel, "Micrornas: genomics, biogenesis, mechanism, and function," cell, vol. 116, no. 2, pp. 281–297, 2004.
[4] S. Wang, T. Liu, C. Ren, W. Wu, Z. Zhao, S. Pang, and Y. Zhang, "Predicting potential small molecule–mirna associations utilizing truncated schatten p-norm," Briefings in Bioinformatics, vol. 24, no. 4, p. bbad234, 2023.
[5] K. Nemeth, R. Bayraktar, M. Ferracin, and G. A. Calin, "Non-coding rnas in disease: from mechanisms to therapeutics," Nature Reviews Genetics, vol. 25, no. 3, pp. 211–232, 2024.
[6] S. Yu, Y. Li, X. Lu, Z. Han, C. Li, X. Yuan, and D. Guo, "The regulatory role of mirna and lncrna on autophagy in diabetic nephropathy," Cellular Signalling, vol. 118, p. 111144, 2024.
[7] S. Suwardjo, K. G. Permana, T. Aryandono, D. S. Heriyanto, and S. L. Anwar, "Long-noncoding-rna hotair upregulation is associated with poor breast cancer outcome: A systematic review and meta analysis," Asian Pacific Journal of Cancer Prevention, vol. 25, no. 4, pp. 1169–1182, 2024.
[8] S. Wang, Z. Zheng, X. Wang, Q. Zhang, and Z. Liu, "A cloud-edge collaboration framework for cancer survival prediction to develop medical consumer electronic devices," IEEE Transactions on Consumer Electronics, 2024.
[9] N. A. Wani, J. Bedi, R. Kumar, M. A. Khan, and I. Rida, "Synergizing fusion modelling for accurate cardiac prediction through explainable artificial intelligence," IEEE Transactions on Consumer Electronics, 2024.
[10] J. Xiao, J. Li, and H. Gao, "Fs3dciot: A few-shot incremental learning network for skin disease differential diagnosis in the consumer iot," IEEE Transactions on Consumer Electronics, 2023.
[11] B. Choudhuri, B. Bhowmick et al., "Design of dual-band rectifier circuit for rf energy harvesting using double-gate graphene nanoribbon (gnr) vertical tunnel fet," IEEE Transactions on Consumer Electronics, 2023.
[12] M.-T. Chen and C.-M. Lin, "Standby power management of a smart home appliance by using energy saving system with active loading feature identification," IEEE Transactions on Consumer Electronics, vol. 65, no. 1, pp. 11–17, 2018.
[13] R. Teng and T. Yamazaki, "Load profile-based coordination of appliances in a smart home," IEEE Transactions on Consumer Electronics, vol. 65, no. 1, pp. 38–46, 2018.
[14] S. Pattanaik, C. Chakraborty, S. Behera, S. K. Majhi, and S. K. Pani, "A miot framework of consumer technology for medical diseases prediction," IEEE Transactions on Consumer Electronics, 2024.
[15] K. Doulani, A. Rajput, A. Hazra, M. Adhikari, and A. K. Singh, "Explainable ai for communicable disease prediction and sustainable living: Implications for consumer electronics," IEEE Transactions on Consumer Electronics, 2023.
[16] M.-M. Yin, Y.-L. Gao, C.-H. Zheng, and J.-X. Liu, "Ntbirw: a novel neighbor model based on two-tier bi-random walk for predicting potential disease-related microbes," IEEE Journal of Biomedical and Health Informatics, vol. 27, no. 3, pp. 1644–1653, 2023.
[17] C. Yan, G. Duan, F.-X. Wu, Y. Pan, and J. Wang, "Brwmda: Predicting microbe-disease associations based on similarities and bi-random walk on disease and microbe networks," IEEE/ACM transactions on computational biology and bioinformatics, vol. 17, no. 5, pp. 1595–1604, 2019.
[18] H.-b. Yao, Z.-j. Hou, W.-g. Zhang, H. Li, and Y. Chen, "Prediction of microrna-disease potential association based on sparse learning and multilayer random walks," Journal of Computational Biology, 2024.
[19] P. Xuan, K. Han, Y. Guo, J. Li, X. Li, Y. Zhong, Z. Zhang, and J. Ding, "Prediction of potential disease-associated micrornas based on random walk," Bioinformatics, vol. 31, no. 11, pp. 1805–1815, 2015.
[20] S. Wang, T. Liu, C. Ren, Y. Zhao, S. Qiao, Y. Zhang, and S. Pang, "Heterogeneous graph inference with range constrainted l2, 1-collaborative matrix factorization for small molecule-mirna association prediction," Computational Biology and Chemistry, vol. 110, p. 108078, 2024.
[21] S.-H. Wang, C.-C. Wang, L. Huang, L.-Y. Miao, and X. Chen, "Dual-network collaborative matrix factorization for predicting small molecule-mirna associations," Briefings in Bioinformatics, vol. 23, no. 1, p. bbab500, 2022.
[22] J. Xu, L. Cai, B. Liao, W. Zhu, P. Wang, Y. Meng, J. Lang, G. Tian, and J. Yang, "Identifying potential mirnas–disease associations with probability matrix factorization," Frontiers in genetics, vol. 10, p. 1234, 2019.
[23] M. Lian, X. Wang, and W. Du, "Integrated multi-similarity fusion and heterogeneous graph inference for drug-target interaction prediction," Neurocomputing, vol. 500, pp. 1–12, 2022.
[24] J. Yin, X. Chen, C.-C. Wang, Y. Zhao, and Y.-Z. Sun, "Prediction of small molecule–microrna associations by sparse learning and heterogeneous graph inference," Molecular pharmaceutics, vol. 16, no. 7, pp. 3157–3166, 2019.
[25] A. Toprak, "circrna-disease association prediction with an improved unbalanced bi-random walk," Journal of Radiation Research and Applied Sciences, vol. 17, no. 2, p. 100858, 2024.
[26] S. Wang, T. Liu, C. Ren, W. Wu, Z. Zhao, S. Pang, and Y. Zhang, "Predicting potential small molecule–mirna associations utilizing truncated schatten p-norm," Briefings in Bioinformatics, vol. 24, no. 4, p. bbad234, 2023.
[27] M.-M. Yin, J.-X. Liu, Y.-L. Gao, X.-Z. Kong, and C.-H. Zheng, "Ncplp: a novel approach for predicting microbe-associated diseases with network consistency

projection and label propagation," IEEE Transactions on Cybernetics, vol. 52, no. 6, pp. 5079–5087, 2020.
[28] M.-M. Yin, Y.-L. Gao, J. Shang, C.-H. Zheng, and J.-X. Liu, "Multi-similarity fusion-based label propagation for predicting microbes potentially associated with diseases," Future Generation Computer Systems, vol. 134, pp. 247–255, 2022.
[29] D. L. Donoho et al., "High-dimensional data analysis: The curses and blessings of dimensionality," AMS math challenges lecture, vol. 1, no. 2000, p. 32, 2000.
[30] J. Gong, W. Liu, J. Zhang, X. Miao, and A.-Y. Guo, "lncrnasnp: a database of snps in lncrnas and their potential functions in human and mouse," Nucleic acids research, vol. 43, no. D1, pp. D181–D186, 2015.
[31] X. Liu, S. Wang, F. Meng, J. Wang, Y. Zhang, E. Dai, X. Yu, X. Li, and W. Jiang, "Sm2mir: a database of the experimentally validated small molecules effects on microrna expression," Bioinformatics, vol. 29, no. 3, pp. 409–411, 2013.
[32] Y. Li, C. Qiu, J. Tu, B. Geng, J. Yang, T. Jiang, and Q. Cui, "Hmdd v2. 0: a database for experimentally supported human microrna and disease associations," Nucleic acids research, vol. 42, no. D1, pp. D1070–D1074, 2014.
[33] L. Wong, L. Wang, Z.-H. You, C.-A. Yuan, Y.-A. Huang, and M.-Y. Cao, "Gklomli: a link prediction model for inferring mirna–lncrna interactions by using gaussian kernel-based method on network profile and linear optimization algorithm," BMC bioinformatics, vol. 24, no. 1, p. 188, 2023.
[34] Z. Yu, F. Zhu, G. Tian, and H. Wang, "Lcbni: link completion bipartite network inference for predicting new lncrna-mirna interactions," in 2018 IEEE International Conference of Safety Produce Informatization (IICSPI). IEEE, 2018, pp. 873–877.
[35] L. Wong, Y.-A. Huang, Z.-H. You, Z.-H. Chen, and M.-Y. Cao, "Lnrlmi: Linear neighbour representation for predicting lncrna-mirna interactions," Journal of cellular and molecular medicine, vol. 24, no. 1, pp. 79–87, 2020.
[36] P. Hu, Y.-A. Huang, K. C. Chan, and Z.-H. You, "Learning multimodal networks from heterogeneous data for prediction of lncrna–mirna interactions," IEEE/ACM Transactions on Computational Biology and Bioinformatics, vol. 17, no. 5, pp. 1516–1524, 2019.
[37] ——, "Discovering an integrated network in heterogeneous data for predicting lncrna-mirna interactions," in Intelligent Computing Theories and Application: 14th International Conference, ICIC 2018, Wuhan, China, August 15-18, 2018, Proceedings, Part I 14. Springer, 2018, pp. 539–545.
[38] Y.-A. Huang, K. C. Chan, and Z.-H. You, "Constructing prediction models from expression profiles for large scale lncrna–mirna interaction profiling," Bioinformatics, vol. 34, no. 5, pp. 812–819, 2018.
[39] S. Wang, T. Liu, C. Ren, W. Wu, Z. Zhao, S. Pang, and Y. Zhang, "Predicting potential small molecule–mirna associations utilizing truncated schatten p-norm," Briefings in Bioinformatics, vol. 24, no. 4, p. bbad234, 2023.
[40] Y. Zhao, X. Chen, J. Yin, and J. Qu, "Snmfsmma: using symmetric nonnegative matrix factorization and kronecker regularized least squares to predict potential small molecule-microrna association," RNA biology, vol. 17, no. 2, pp. 281–291, 2020.
[41] S.-H. Wang, C.-C. Wang, L. Huang, L.-Y. Miao, and X. Chen, "Dual-network collaborative matrix factorization for predicting small molecule-mirna associations," Briefings in Bioinformatics, vol. 23, no. 1, p. bbab500, 2022.
[42] X. Chen, C. Zhou, C.-C. Wang, and Y. Zhao, "Predicting potential small molecule–mirna associations based on bounded nuclear norm regularization," Briefings in Bioinformatics, vol. 22, no. 6, p. bbab328, 2021.
[43] N.-N. Guan, Y.-Z. Sun, Z. Ming, J.-Q. Li, and X. Chen, "Prediction of potential small molecule-associated micrornas using graphlet interaction," Frontiers in pharmacology, vol. 9, p. 1152, 2018.
[44] D. Ouyang, Y. Liang, J. Wang, L. Li, N. Ai, J. Feng, S. Lu, S. Liao, X. Liu, and S. Xie, "Hgclamir: Hypergraph contrastive learning with attention mechanism and integrated multi-view representation for predicting mirna-disease associations," PLOS Computational Biology, vol. 20, no. 4, p. e1011927, 2024.
[45] Y. Rao, M. Xie, and H. Wang, "Predict potential mirna-disease associations based on bounded nuclear norm regularization," Frontiers in Genetics, vol. 13, p. 978975, 2022.
[46] S. Li, M. Xie, and X. Liu, "A novel approach based on bipartite network recommendation and katz model to predict potential micro-disease associations," Frontiers in Genetics, vol. 10, p. 485914, 2019.
[47] G. Xie, Z. Fan, Y. Sun, C. Wu, and L. Ma, "Wbnpmd: weighted bipartite network projection for microrna-disease association prediction," Journal of translational medicine, vol. 17, pp. 1–11, 2019.
[48] J. Xu, L. Cai, B. Liao, W. Zhu, P. Wang, Y. Meng, J. Lang, G. Tian, and J. Yang, "Identifying potential mirnas–disease associations with probability matrix factorization," Frontiers in genetics, vol. 10, p. 1234, 2019.
[49] X. Chen, L. Wang, J. Qu, N.-N. Guan, and J.-Q. Li, "Predicting mirna–disease association based on inductive matrix completion," Bioinformatics, vol. 34, no. 24, pp. 4256–4265, 2018.